

Alma Mater Studiorum Università di Bologna
Archivio istituzionale della ricerca

Water sorption in microfibrillated cellulose (MFC): The effect of temperature and pretreatment

This is the final peer-reviewed author's accepted manuscript (postprint) of the following publication:

Published Version:

Meriçer, Ç., Minelli, M., Giacinti Baschetti, M., Lindström, T. (2017). Water sorption in microfibrillated cellulose (MFC): The effect of temperature and pretreatment. CARBOHYDRATE POLYMERS, 174, 1201-1212 [10.1016/j.carbpol.2017.07.023].

Availability:

This version is available at: <https://hdl.handle.net/11585/615471> since: 2018-01-15

Published:

DOI: <http://doi.org/10.1016/j.carbpol.2017.07.023>

Terms of use:

Some rights reserved. The terms and conditions for the reuse of this version of the manuscript are specified in the publishing policy. For all terms of use and more information see the publisher's website.

This item was downloaded from IRIS Università di Bologna (<https://cris.unibo.it/>).
When citing, please refer to the published version.

(Article begins on next page)

This is the final peer-reviewed accepted manuscript of:

*Çağlar Meriçer, Matteo Minelli, Marco Giacinti Baschetti, Tom Lindström, **Water sorption in microfibrillated cellulose (MFC): The effect of temperature and pretreatment**, Carbohydrate Polymers, Volume 174, 2017, Pages 1201-1212, ISSN 0144-8617*

The final published version is available online at:

<https://doi.org/10.1016/j.carbpol.2017.07.023>

Rights / License:

The terms and conditions for the reuse of this version of the manuscript are specified in the publishing policy. For all terms of use and more information see the publisher's website.

This item was downloaded from IRIS Università di Bologna (<https://cris.unibo.it/>)

When citing, please refer to the published version.

1 Water sorption in microfibrillated cellulose (MFC): The effect of temperature
2 and pretreatment

3
4 Çağlar Meriçer^a, Matteo Minelli^a, Marco Giacinti Baschetti^{*, a}

5 T. Lindström^b,

6 ^a *Dipartimento di Ingegneria Civile, Chimica, Ambientale e dei Materiali (DICAM) -*
7 *Università degli studi di Bologna, via Terracini 28, 40131 - Bologna (Italy)*

8 ^b *Innventia AB, Box 5604, SE-11486 Stockholm, Sweden*

9 (To Be submitted to Carbohydrate Polymers)

10
11 **Keywords:** Nanocellulose; Water sorption; Solubility isotherm; Sorption modeling

12
13 **Highlights:**

- 14 • Water solubility is measured on different microfibrillated cellulose (MFC) films
- 15 • The effect of temperature on water sorption is investigated in the range 16-65 °C
- 16 • Water uptake results higher in carboxymethylated MFC than enzymatic MFC
- 17
- 18
- 19

20 **Corresponding author**

21 Marco Giacinti B.

22 Tel. +39 (0) 51 2090408

23 Fax +39 (0) 51 2090247

24 marco.giacinti@unibo.it

Abstract

Water sorption behavior of two different microfibrillated cellulose (MFC) films, produced by delamination of cellulose pulp after different pretreatment methods, is examined at various temperatures (16 - 65 °C) and up to 70% RH. The effect of drying temperature of MFC films on the water uptake is also investigated.

The obtained solubility isotherms showed the typical downward curvature at moderate RH, while no upturn is observed at higher RH; the uptakes are in line with characteristic values for cellulose fibers. Enzymatically pretreated MFC dispersion showed lower solubility than carboxymethylated MFC, likely due to the different material structure, which results from the different preparation methods. The experimental results are analyzed by Park and GAB models, which proved suitable to describe the observed behaviors.

Interestingly, while no significant thermal effect is detected on water solubility above 35 °C, the uptake at 16 and 25 °C, at a given RH, is substantially lower than that at higher temperature, indicating that, in such range, sorption process is endothermic. Such unusual behavior for a cellulose-based system seems to be related mainly to the structural characteristics of MFC films, and to relaxation phenomena taking place upon water sorption.

The diffusion kinetics, indeed, showed a clear Fickian behavior at low temperature and RH, whereas a secondary process seems to occur at high temperature and higher RH, leading to anomalous diffusion behaviors.

1. Introduction

Recently, there has been a growing interest in bio-based materials due to their high level of sustainability, biodegradability and recyclability. Petroleum-based products, still highly utilized for many different applications, are indeed responsible for serious environmental issues that push towards alternative and more environmental friendly solutions such as those offered by bio-based materials (Johansson et al., 2012). Among many possible choices, cellulose, the most abundant organic polymer on Earth, is a perfect candidate for such replacement, being already widely used for various purposes, and, among the others, for packaging applications. However, the most typical cellulose derivatives, namely paper and paperboard, lack many of the properties required to replace oil-based plastics, such as water resistance, formability, and gas and moisture barrier. For these reasons, relevant research efforts during the last decades have been devoted to the processing and the modification of cellulose to produce novel derivatives with significantly improved performances with respect to conventional paper or paperboard products and unaltered biodegradability.

In this concern, the development of nano-sized cellulosic materials, as microfibrillated cellulose, MFC (also referred as nanofibrillated cellulose, NFC), nanowhiskers or nanocrystals, disclosed new opportunities in the use of cellulose for packaging applications, due to their peculiar features, including a remarkable gas and oil barrier properties (Berglund, 2005; Dufresne, 1998; Azizi Samir, Alloin, & Dufresne, 2005; Kamel, 2007; Dufresne, 2008; Hubbe, Rojas, Lucia, & Sain, 2008; Nogi, Iwamoto, Nakagaito, & Yano, 2009).

The characteristics and the structural behavior of the different types of nanocellulose may vary due to the different production procedures and protocols. Microfibrillated cellulose, (MFC) is obtained after the mechanical disintegration of the cellulosic fibers from plant cell walls, as first explored by Turbak, Snyder, & Sandberg (1983) and Herrick, Casebier, Hamilton, & Sandberg (1983). The delamination of the fibers, promoted by different types of pretreatment

on the raw pulp, is carried out in a high pressure homogenization process, which, due to high shearing of wood pulp, leads to the formation of elementary fibrils and microfibrils having final width of less than 20 nm and length up to several micrometers (Plackett et al., 2010; Siró, Plackett, Hedenqvist, Ankerfors, & Lindström, 2011; Svagan, Azizi Samir, & Berglund, 2007).

The MFC, produced as highly diluted water dispersion, can be processed to obtain thin films with good stiffness and strength, due to high aspect ratios of the fibrils; MFC is also suitable as reinforcement for the design of novel bionanocomposites with improved mechanical behavior (Henriksson et al., 2008; Leitner et al., 2007; Nogi et al., 2009; Svagan et al., 2007; Syverud & Stenius, 2009, Iwatake, Nogi, & Yano (2008), Zimmermann, Pöhler, & Geiger (2004)). Furthermore, the large amount of hydroxyl groups onto the microfibrils surface provides available sites for chemical modifications and for functionalization of the cellulosic materials for various applications (e.g. the hydrophobization) (Lu, Askeland, & Drzal, 2008; Siqueira, Bras, & Dufresne, 2009; Stenstad, Andresen, Tanem, & Stenius, 2008, Andresen et al. (2007)).

The large crystalline content of MFC (Aulin et al., 2009; Lu, Wang, & Drzal, 2008), and its ability to form dense networks by strong interfibrillar hydrogen bonds, provides excellent gas barrier properties to MFC films, suitable for nanocomposites and coating formulations for barrier packaging applications (Fukuzumi et al., 2009; Syverud & Stenius, 2009). Syverud & Stenius (2009) measured the oxygen barrier properties of 21 μm -thick MFC films produced from bleached spruce sulfite pulp at 23 °C and 0% RH, and reported a permeability of $1.9 \cdot 10^{-18} \text{ mol m/m}^2 \text{ s Pa}$, comparable with well-known ultra-barrier oil-based materials such as polyvinyl alcohol, PVOH ($1.0 \cdot 10^{-19} \text{ mol m/m}^2 \text{ s Pa}$) or polyvinylidene chloride, PVdC ($7.9 \cdot 10^{-19} \text{ mol m/m}^2 \text{ s Pa}$) (Lange & Wyser, 2003). Alternatively, Fukuzumi et al. (2009) prepared an MFC (TEMPO oxidized softwood and hardwood pulps) thin coating, 0.4 μm , on plasma-treated PLA film, leading to a dramatic reduction of the oxygen transfer rate. Minelli et al.

(2010) characterized the barrier properties of the two MFC types investigated in this work and obtained permeability values equal to $2.6 \cdot 10^{-19}$ and $6.3 \cdot 10^{-19}$ mol m/m² s Pa for enzymatically pretreated MFC and carboxymethylated MFC, respectively. Plackett et al. (2010) coupled the same MFC materials with amylopectin, obtaining a further decrease of the oxygen permeability values for a 50/50 MFC/amylopectin composite films. MFC has been also used in combination with different inorganic fillers aiming at the fabrication of nanocomposites with improved barrier properties; among the others, Liu et al. (2011), prepared composite materials with 50/50 weight composition of MFC and clay, claiming an extraordinary low ($5.0 \cdot 10^{-21}$ mol m/ m² s Pa) oxygen permeability in dry conditions.

Despite the very promising results obtained in dry conditions, the large number of hydroxyl groups onto MFC fibrils surface causes a strong sensitivity of cellulosic materials to moisture, with a consequent worsening of the material properties, including also the reduction of the oxygen barrier ability under humid environments. Indeed, moisture uptake causes structural changes in cellulosic substrates, visible from the changes of appearance, and resulting in remarkably altered materials properties (Siroka, Noisternig, Griesser, & Bechtold, 2008). This drawback has been studied extensively, and the effect of humidity on the oxygen permeability of MFC films has been quantitatively evaluated (Aulin, Gällstedt, & Lindström, 2010; Minelli et al., 2010; Österberg et al., 2013). Minelli et al. (2010) and Aulin et al. (2010) observed a two-step increase of the oxygen permeability in MFC films, with an initial rise of two orders of magnitude, followed by a sort of plateau up to a water activity of about 60-70% RH, corresponding to about 10-15 wt. % of water in the MFC matrix; a further increase is finally observed above 80% of RH. Interestingly, Österberg et al. (2013) developed a simple preparation method based on pressure filtration for MFC films and with improved resistance toward moisture at intermediate water activities; however, the sharp increase of O₂ permeability at very high RH still remains a challenge.

Clearly, the large water uptake by the cellulose nanofibers produces a significant swelling of MFC film that leads to a large plasticization of the matrix, eventually enhancing the gas permeability. However, in spite of a large number of experimental and modeling analyses, the deep understanding of these mechanisms is still undisclosed (Belbekhouche et al., 2011; Bessadok et al., 2009; Gouanvé et al., 2007; Minelli et al., 2010; Österberg et al., 2013).

Current view for cellulosic materials relies on the idea that water molecules are not simply adsorbed onto the fibrils surface, but are also able to penetrate into the amorphous part of cellulose structure, leading to larger water uptakes, exceeding the contribution given by the specific surface area of the material (Zografi, Kontny, Yang, & Brenner, 1984). Previous studies on cellulose powders investigated the influence of material properties such as crystallinity fraction, surface area and pore volume on the interaction with moisture, and concluded that the moisture uptake is higher for materials with a lower crystallinity index (i.e. a larger amorphous portion), higher pore volume and surface area (Kohler et al., 2003; Mihranyan et al., 2004; Okubayashi et al., 2004). Belbekhouche et al. (2011) compared the water vapor sorption behavior in cellulose whiskers and MFC produced from sisal, obtaining approximately the same water uptake, as a direct consequence of the same amount of amorphous regions of the two systems, although different morphologies were observed. Related studies claimed that the water diffuses first towards the amorphous regions, and the external sites of the fibrils, which are more accessible and available for water molecules, whereas the sites at the inner surface and onto the crystallites are involved only when the matrix has been significantly swollen (Belbekhouche et al., 2011; Okubayashi et al., 2004).

In spite of the large amount of work carried out in the water sorption characterization in cellulosic materials, and particularly in MFC, to authors' best knowledge, very limited experimental data are available on the effect of temperature on water solubility. Indeed, only Bedane et al. (2015) investigated water solubility in nanofibrillated cellulose at various

temperatures, limiting however their analysis to the range 5 to 35 °C. Nevertheless, this peculiar aspect has a significant relevance for practical purposes, being the removal of water from MFC suspensions one of the most critical aspects in the production of nanocellulose based coatings or films. For this reason, in the present study, the water vapor sorption of two types of MFC is presented with the focus on the effect of temperature, and experiments have been carried out spanning over a rather broad range of temperature (16-65 °C) and relative humidity (0-70%). The effect of the drying protocol on the MFC samples on the resulting water solubility is also investigated. The comparison of the moisture uptake is linked to their structural difference and temperature dependence of the solubility modeling parameters is briefly discussed. Further information on the sorption kinetics and the related modeling analysis will be presented in a future article, devoted to the description of the kinetic analysis of water transport in cellulosic materials.

2. Experimental

2.1. Materials

The films investigated in this work have been prepared from aqueous dispersions of MFC (2 wt. %), produced and kindly provided by Innventia AB (Stockholm, Sweden). Two different materials have been investigated, often labeled as MFC generation 1 (MFC G1) and MFC generation 2 (MFC G2), characterized by different pretreatment procedures carried out on the cellulose pulp prior the delamination in the high pressure homogenization step. The detailed procedure for their production as well as the physical and morphological characterizations are reported in previous works (Pääkkö et al., 2007; Wågberg et al., 2008), only a brief description is here included, for the sake of clarity.

Commercial never dried sulfite softwood dissolving pulp (Domsjö Dissolving Plus, Domsjö Fabriker AB, Sweden) has been used for the production of both MFC G1 and MFC G2

dispersions. Prior to the high-pressure homogenization step, 3-5 passes in two differently sized fluidizers in series (Pääkko et al., 2007), the cellulose pulp has been first subjected to a combined refining and enzymatic pre-treatment, resulting in MFC G1 microfibrils with diameters of ~17–30 nm and charge density of ~40 $\mu\text{equiv/g}$ (Fukuzumi et al., 2009). Conversely, the production of MFC G2 has been carried out by the carboxymethylation of the cellulose pulp, followed by a high-pressure homogenization step at 1650 bar, passing one time through the fluidizer with two different chambers in series. Such process allowed to obtain microfibrils with smaller diameters, in the range of 5–15 nm, and higher surface charge, ~586 $\mu\text{equiv/g}$ (Wågberg et al., 2008).

Pure MFC G1 and MFC G2 films have been prepared by solution casting of the MFC water dispersions, following the procedure already described in previous studies (Minelli et al., 2010; Plackett et al., 2010). The MFC dispersions have been first diluted by deionized water in order to prepare a suspension that could be easily poured (1% of solid content for MFC G1, and 0.7% for MFC G2), vigorously stirred for about 3 h, and then poured into a glass Petri dish. The films have been obtained after the water evaporation in a clean hood at ambient conditions. The films thickness has been measured by a Mitutoyo micrometer (Mitutoyo Scandinavia AB, Väsby, Sweden) in 10 different spots, resulting in average values ranging from 18 to 25 μm with an absolute error of $\pm 1 \mu\text{m}$ for both materials.

Ultra-pure, double distilled water (Carlo Erba, conductivity lower than 0.01 $\mu\text{S/cm}$), has been used as penetrant during all the experiments.

2.2. Moisture Sorption

The experimental device used for water sorption tests is a classical pressure decay apparatus (Fig. 1), already described elsewhere (Minelli, De Angelis, Doghieri, Rocchetti, & Montenero, 2010), in which the penetrant uptake is evaluated by a manometric measure in a

closed cell, whose volume has been conveniently calibrated. The apparatus has two identical branches in order to be able to test two different samples at the same time.

The specimens are first placed in the sample cell, and then conditioned under vacuum for at least 24 h, in order to remove absorbed atmospheric moisture, at the desired test temperature. In this case, at the lowest temperatures inspected (below 35 °C), preliminary experiments revealed the presence of residual water, so that the samples have been also dried at higher T values, in order to ensure complete water removal, as it will better explained in the results section. After the pretreatment, the pre-chamber is loaded by water vapor at a certain activity, and when the pressure reached a stable value, the sorption experiment started by opening the valve between the pre-chamber and sample chamber (V05 and V07 in Fig. 1). After a sudden pressure drop due to volume expansion in the very first few seconds, an asymptotic decrease of pressure, due to the sorption in the MFC film is observed, and measured, in order to obtain information on the sorption process.

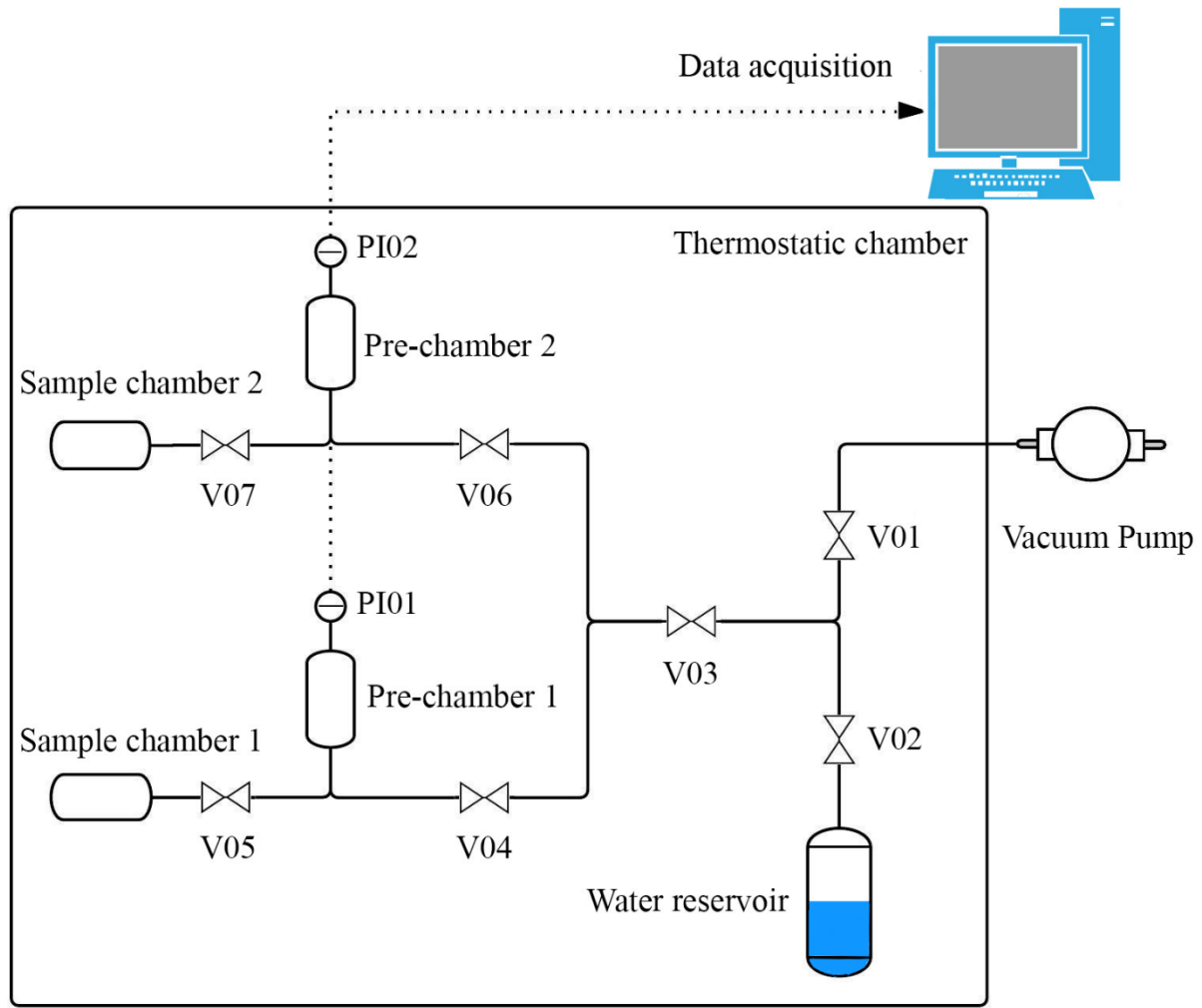


Figure 1. Layout of the pressure decay apparatus.

The procedure is applied by increasing stepwise the pressure, after the final equilibrium of the previous step is reached, in order to explore a wide range of penetrant activity and to determine the solubility isotherm at the given experimental temperature. The amount of water absorbed in the MFC films is then calculated from the pressure decrease by means of a suitable equation of state (e.g. ideal gas law, as in the present case), being the chamber volume accurately known. The water uptake at the i^{th} step, expressed as mass ratio Ω_w^i , i.e mass of water per the mass of MFC m_{MFC} , is calculated by Eq. (1) below, in which p_0^i and p_∞^i are the initial and final water vapor pressures respectively, V is the sample chamber volume and M_w is the penetrant molar mass:

$$\Omega_w^i = \Omega_w^{i-1} + \frac{(p_0^i - p_\infty^i) V M_w}{R T m_{MFC}} \quad (1)$$

Sorption kinetics can also be evaluated in the same tests by processing the experimentally measured mass uptake as a function of time through the use of Fick's law with the appropriate boundary conditions. Eq. (2) below, proposed by Crank (1956), provides the relative water uptake in the i^{th} sorption step as a function of time:

$$\frac{\Omega_w^i(t) - \Omega_w^{i-1}}{\Omega_w^i - \Omega_w^{i-1}} = 1 - \sum_{n=1}^{\infty} \frac{2\alpha(1+\alpha)}{1+\alpha+\alpha^2 q_n^2} e^{-D q_n^2 t/l^2} \quad (2)$$

in which Ω_w^{i-1} and Ω_w^i are the initial and final penetrant mass ratio of the i^{th} sorption step, q_n are the positive solutions of the equation $\tan(q_n) = -\alpha q_n$, being α the dimensional length obtained by the ratio $A/(Kl)$ between sample area (A), its thickness (l), and the water partition coefficient between the membrane and the vapor phase (K). The Fickian diffusion coefficient (D), assumed constant during each experimental sorption step, is the only unknown in Eq. (2), and it can be obtained by the best fit of the experimental kinetic data.

Sorption experiments have been carried out at 16, 25, 35, 45, 55 and 65 °C, for both MFC G1 and MFC G2, and in water activity range spanning from 0 to 70% RH. Higher relative humidity could not be investigated due to intrinsic limitations of the experimental technique employed.

3. Modeling background

The solubility of water in cellulose-based materials has been analyzed by a variety of suitable approaches, and different models have been reported as effective in representing the solubility and swelling isotherms, and able to account for significant interactions between water molecules and the cellulosic matrix.

Similar to most of the hydrophilic materials, the water sorption in MFC typically shows a type II isotherm according to the IUPAC classification (Rouquerou et al., 1994), characteristic for non-porous or microporous materials, with an initial downward curvature (Langmuir), and an upturn at high activities usually associated to clustering or multilayer adsorption. Such behavior is the result of different sorption processes occurring on external cellulose hydroxyl groups, in the interfibrillar amorphous regions, and onto micro-voids and crystallites. Furthermore, water molecules can also be directly adsorbed on the water molecules already bound to the fiber (Morton & Hearle, 1993). According to Kohler et al. (2003), water molecules have easier access into the areas between the fibrils and bundles compared to the free volume inside the fibrils.

Three different approaches are mainly considered to describe water solubility in nanocellulose (and in cellulosic materials in general), as reviewed by Belbekhouche et al. (2011):

i) physical adsorption of water as a single layer on the surface of crystalline domains, modeled through a Langmuir type isotherm;

ii) physical multilayer sorption, in which water can be adsorbed directly on crystal sites or on water molecules already adsorbed, as described by specific models, such as the BET theory (Brunauer, Emmett, & Teller, 1938), or the GAB model (Guggenheim, 1966);

iii) empirical or semi-empirical models, developed for an accurate fitting of the experimental behavior, but in lack of any physical meaning (see e.g. Ferro-Fontan, Chirife, Sancho & Iglesias, 1982; Henderson, 1952; Smith, 1947; Oswin, 1946; Peleg, 1993; Halsey, 1948; Al-Muhtaseb, McMinn, & Magee, 2004; Belbekhouche et al., 2011).

Water sorption in cellulosic materials is often well described also by Park model (Park, 1986), even at high R.H., considering different contributions to water sorption, and allowing for both physical adsorption and water dissolution in the cellulosic matrix. GAB and Park

models are widely employed to describe the water solubility in cellulose based materials (Alix et al., 2009; Bessadok et al., 2007; Gouanvé et al., 2006, 2007), and also in nanosized cellulose (Belbekhouche et al., 2011; Minelli et al., 2010), due to their ability to describe well the experimental behaviors and for the physical meaning of the model parameters. Hence, the GAB and Park are considered for the description of water solubility isotherms obtained in this work, aiming at a more thorough comprehension of the process. A brief description of the two models is given in the following sections.

3.1. Park Model

The Park model (1986) is based on the dual mode sorption idea, in which a Langmuir-type adsorption (A_L : Langmuir capacity constant, b_L : Langmuir affinity constant) is combined with an ordinary dissolution (absorption) described by Henry's law (K_H : Henry's solubility coefficient) (Michaels, Vieth, & Barrie, 1963; Vieth & Sladek, 1965). A third contribution is then introduced to account for water clustering, involving multiple (n) self-associated water molecules inside the matrix, occurring mainly at high water activity (usually above 70-80% R.H.). This term in particular is described by two further parameter, K_a , a sort of equilibrium constant for the clustering mechanism, and the number of molecules forming the cluster, n .

The total water uptake in the cellulose based materials (expressed as mass fraction, Ω_w) is the sum of the different contributions and includes 5 model parameters.

$$\Omega_w^{Park} = \Omega_w^L + \Omega_w^H + \Omega_w^c = \frac{A_L b_L a_w}{1 + b_L a_w} + K_H a_w + K_a n a_w^n \quad (3)$$

As the very high RH values were not explored in this work, the clustering term is not considered, and Eq. (3) becomes the traditional dual mode sorption equation, in which the slope of the linear part of the solubility isotherm gives Henry's coefficient K_H , whereas A_L and b_L are determined from the intercept after linearization of the relevant terms.

3.2. GAB Model

The Guggenheim–Anderson–de Boer (GAB) model (Guggenheim, 1966) describes the water uptake as the adsorption of the penetrant molecules layer by layer on the available sites in the cellulose material. It has been derived considering that the active sorption sites are identical, and subsequent layers are characterized by lower interaction energies values comprised between those of the monolayer molecules and that of the bulk liquid. (Quirijns, Van Boxtel, Van Loon, & Van Straten, 2005). Two main parameters are defined, namely the penetrant adsorption capacity C_m in the solid adsorbed onto a monolayer and the constant K_{ads} , referred to the adsorption enthalpy difference between multilayer water molecules and bulk liquid state describing the degree of localized sorption. A third parameter, the Guggenheim constant C_G , included in the Eq. (4), measures the strength of bound water to the primary binding sites; it represents the ratio of the partition function of the first molecule sorbed on a site and the partition function of molecules sorbed at the outer layers. The water uptake is then obtained as:

$$\Omega_w^{GAB} = \frac{C_M C_G K_{ads} a_w}{(1 - K_{ads} a_w)(1 - K_{ads} a_w + C_G K_{ads} a_w)} \quad (4)$$

4. Results and discussion

Differential water sorption experiments have been carried out on two different MFC materials in the temperature range from 16 to 65 °C, and up to approximately 0.70 of water activity, allowing the determination of the water solubility isotherms and the evaluation of the kinetic characteristics.

4.1. Steady state solubility

The results obtained from sorption experiments at different temperatures are reported in Fig. 2 (MFC G1) and Fig. 3 (MFC G2), which illustrate, at all temperatures investigated, the typical solubility behavior observed for water vapor in cellulosic materials (Belbekhouche et

al., 2011), with a clear downward curvature in the low activity range, and a linear trend at intermediate R.H. values. Interestingly, no upturn of the solubility isotherms has been observed, as the limit of very high activities (i.e. above 0.80) has not been explored in the present study. Water solubility at all temperatures is reported in term of water to MFC mass ratio Ω_w as function of water activity (that is the ratio between water pressure in the vapor phase and water vapor pressure, $p/p^*(T)$). Fig. 4 compares the solubility isotherms at 35 °C obtained in this work, with analogous data available in the open literature for other types of nanocellulose materials.

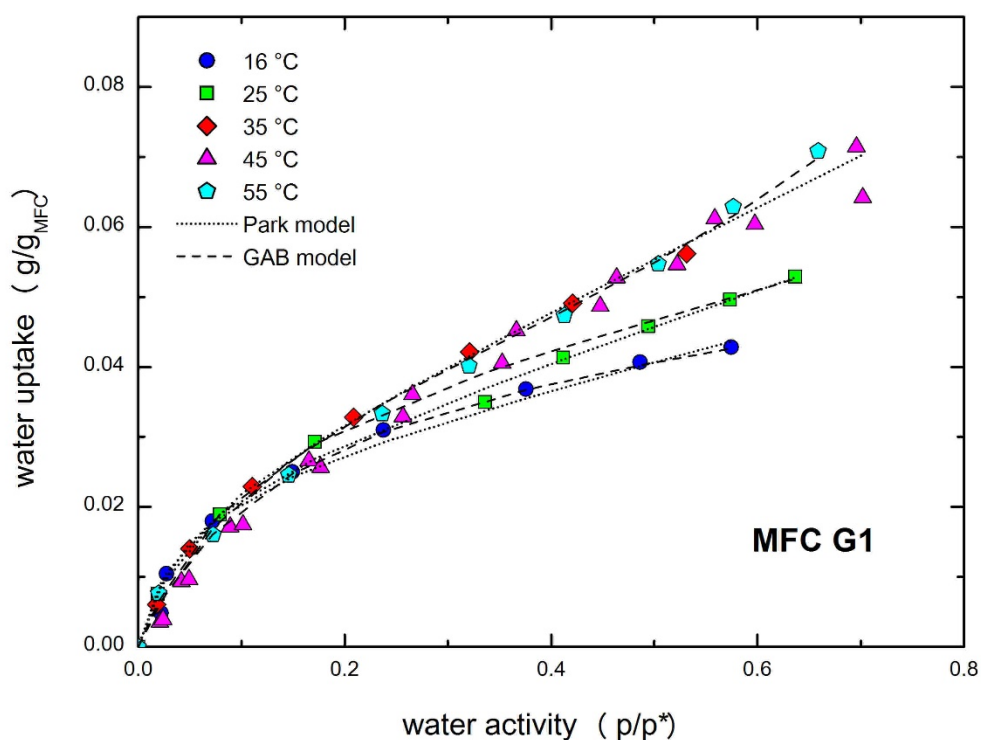


Figure 2. Water solubility isotherms in MFC G1: experimental data and model curves (dotted lines: Park model; and dashed lines GAB model).

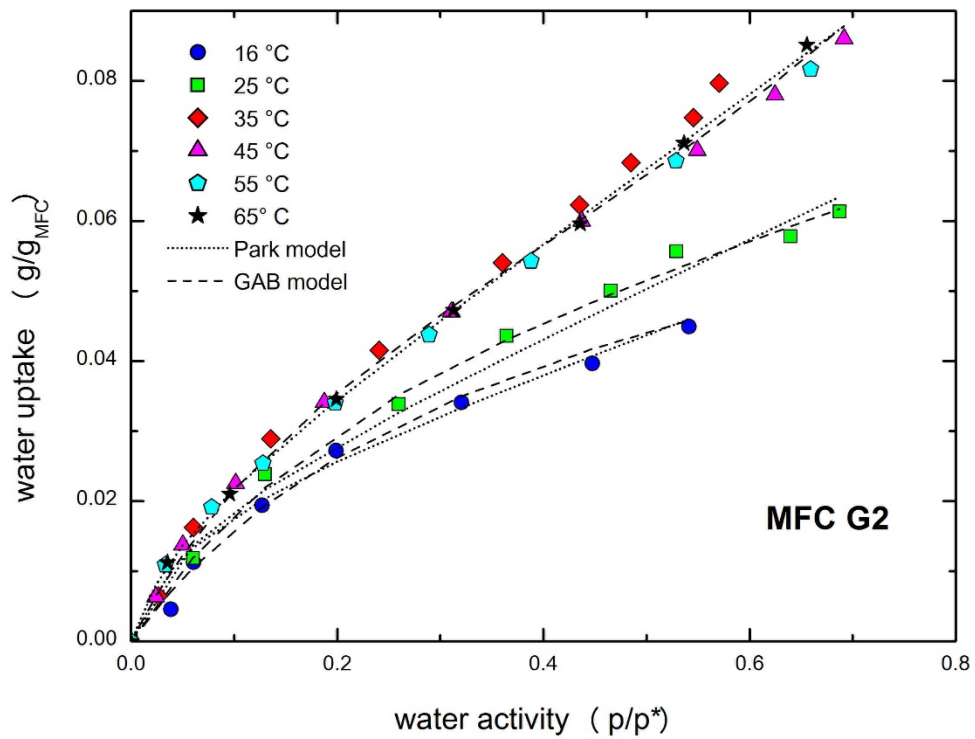


Figure 3. Water solubility isotherms in MFC G2: experimental data and model curves (dotted lines: Park model; and dashed lines GAB model).

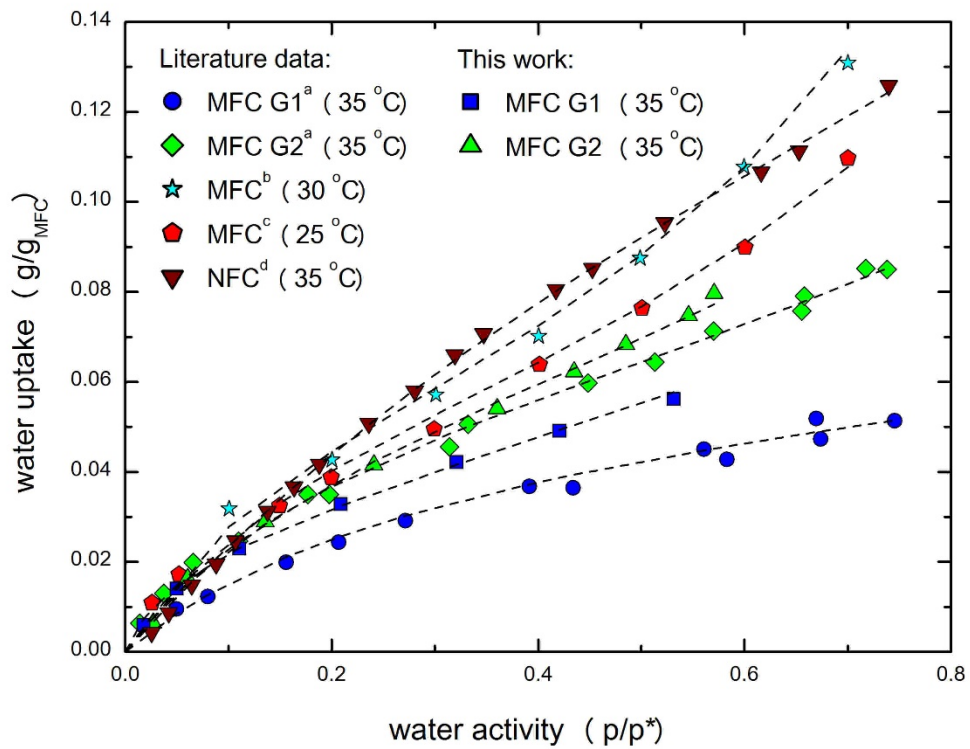


Figure 4. Comparison of water solubility isotherms in nanocellulose with literature data: (a) Minelli et al., 2010; (b) Aulin et al., 2010; (c) Belbekhouche et al., 2011; (d) Bedane et al., 2015.

As can be seen from the figures, a maximum water uptake of 0.070 g/g_{MFC} has been registered for MFC G1 at 70% R.H., while MFC G2 presented a more hydrophilic character, as the penetrant uptake increased up to 0.085 g/g_{MFC} at the same activity. This feature, already observed by Minelli et al. (2010), is related to the different material characteristics, as result of preparation techniques described above. Indeed, the carboxymethylation pretreatment of the cellulose pulp (MFC G2) produced microfibrils with a larger surface charge, and a more accessible interfibrillar region, leading thus to a more pronounced plasticization effect caused by water, even at moderate activities, due to a significant swelling of the cellulose matrix. Interestingly, Österberg et al. (2013) observed that a large number of carboxylic groups promoted during pre-treatments, such as carboxymethylation or TEMPO-mediated oxidation, produces final materials more sensitive towards water and moisture. Indeed, the water solubility in TEMPO nanocellulose reported by Bedane et al. (2015) revealed quite large uptakes, appreciably larger than those obtained in this work.

It also noteworthy that, the more compact and closely packed structure of MFC G1 contributes to lower the water solubility in MFC G1, as also indicated by lower gas permeability observed for this material with respect to MFC G2 (Minelli et al., 2010).

Similarly, as one can see in Fig. 4, the enzymatically pretreated and carboxymethylated MFC showed lower water uptake compared to MFC produced from sisal pulp in the study of Belbekhouche et al. (2011) at 25 °C, with differences that may be ascribed to the different cellulose source and the preparation procedure. Indeed, the pretreatment of the sisal pulp involved several cycles in the homogenizer, resulting in comparably higher fibril diameters (≈50 nm) for sisal MFC, although its crystalline content (75%) is slightly higher than those reported for the materials in this study (63 ± 9%; Aulin et al., 2009). On the other hand, the

method used to fabricate the MFC films and the drying procedure are also relevant in the packing of the fibril structure, determining thus different sorption and permeation properties due to hydrogen bonding, fiber dimensions and void structures (Lavoine, Desloges, Dufresne, & Bras, 2012).

Aulin et al. (2010) also analyzed the water solubility of MFC films obtained using the same source of pulp, which has been carboxymethylated and then homogenized 10 times to produce the final MFC. The resulting material showed the highest water uptake at 30 °C, compared to the others, suggesting that a higher number of homogenization cycles may produce a more homogeneous fibrillated structure and nanofibrils with a larger specific surface area compared to, MFC G2, analyzed in this study, which was produced after one pass only in the fluidizer (Wågberg et al., 2008). Minelli et al. (2010) reported a substantially lower water solubility in MFC G1 with respect to the one obtained here, while data for MGC G2 are very similar. That is related to the different experimental procedure followed in this work, in which the MFC G1 is dried at 45 °C prior the sorption experiment, and not at the operative temperature (35° C) as in the previous study. Such value, indeed, was not sufficient to remove completely the atmospheric moisture from the sample, as will be better discussed in the following section, leading to an apparent lower water uptake.

4.2. Influence of temperature

The analysis of temperature effect on water solubility in MFC films requires to address two aspects. First, in view of strong hydrophilic character of the cellulosic material, the complete removal of the residual water from the MFC sample has to be ensured, prior to any solubility measurement. In this respect, an increase of conditioning temperatures resulted more effective in drying the samples, and ensuring a correct solubility evaluation (De Angelis et al., 2006). Second, the effect of temperature on the penetrant solubility is ascribed to a non-

negligible heat of mixing or to structural relaxation phenomena, which can be revealed by the data analysis.

In order to address the first feature, ad hoc measurements have been carried out preconditioning the MFC samples following different protocols, i.e. drying them at different temperatures (higher than the test temperature), and then running sorption experiments at constant temperature. Interestingly, the resulting sorption behaviors, illustrated in Fig. 5 (MFC G1) and 6 (MFC G2), showed a significant increase of water uptake as the drying temperature is raised, due to a non-negligible effect of the drying temperature on the different types of MFC. Furthermore, above 35 °C for MFC G1 (or 25 °C for MFC G2), no further appreciable difference is observed, suggesting that such temperature is sufficient to obtain repeatable results and ensure the complete removal of the residual atmospheric moisture. As expected, a more intensive drying protocol is able to remove more water, and the resulting solubility is enhanced; the comparison of the two solubility isotherms obtained at 35 °C with different conditioning protocols (Fig. 5) seems to support this analysis, as the final slopes at high R.H. of the two sets of data are very similar, although the absolute solubility values appear quite different. In this concern, the data from Minelli et al. (2010) are also reported in Fig. 5 to show that once the same pretreatment is accounted for, only minor discrepancies are observed, related to the experimental error.

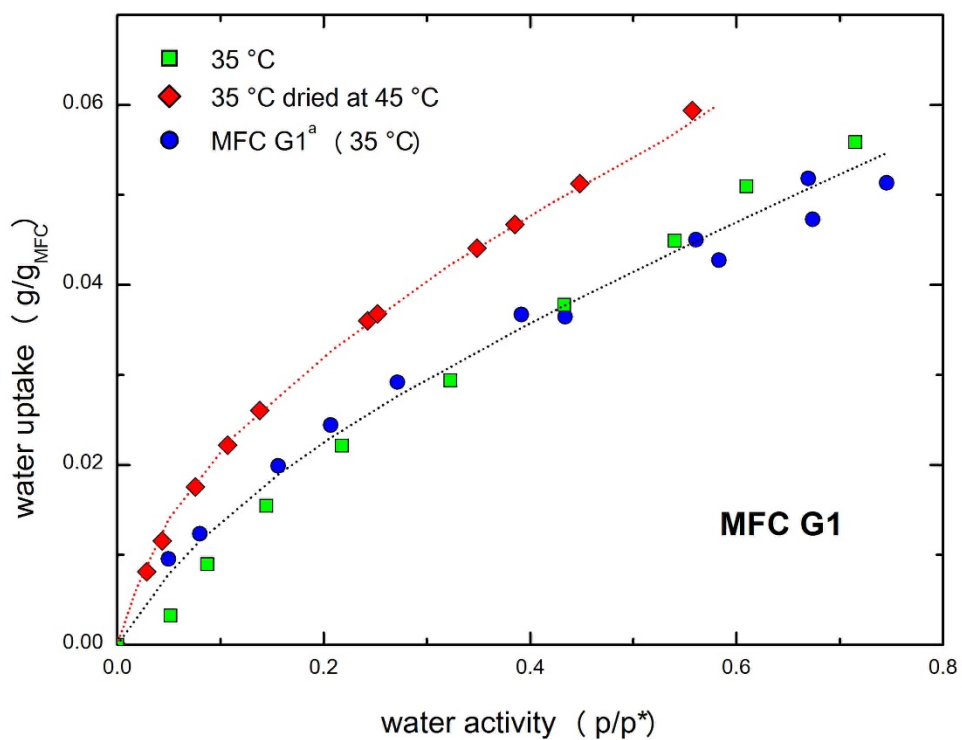


Figure 5. The effect of drying temperature on solubility isotherms for MFC G1 (^a Minelli et al., 2010; dashed lines are drawn to guide the eye).

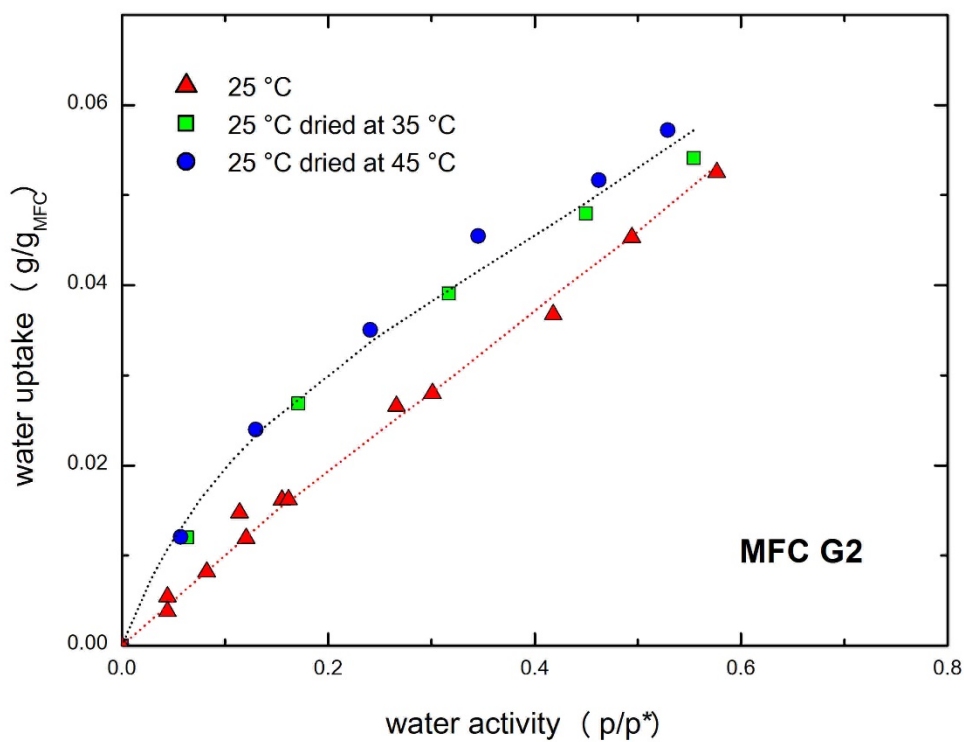


Figure 6. The effect of drying temperature on solubility isotherms for MFC G2 (dashed lines are drawn to guide the eye).

Once the residual water has been conveniently eliminated by appropriate thermal drying pretreatment, as it was carried out for the data reported in Fig. 2 and Fig. 3 previously discussed, a certain discrepancy is still appreciable at the lower temperatures, whereas at higher values the curves are practically superimposed. In particular, as one can see in Fig. 2 and 3, the solubility isotherms at 16 and 25 °C in both MFC G1 and MFC G2 lie appreciably below those at higher temperatures, and the water uptake increases at increasing T. The obtained behavior is quite surprising, as penetrant solubility in polymers typically decreases at increasing temperature, due to the reduction of the binding energy and to the increase in kinetic energy, which enhances the distance among molecules and make less favorable the interaction between the penetrant and the adsorption sites (Quirijns et al., 2005). More specifically, plenty of experimental studies pointed out a decreasing function of water solubility with temperature in many cellulose or cellulose derived materials (see e.g. Jeffries, 1960; Velázquez de la Cruz et al. 2001), and even the raw cellulose pulp used for MFC production of the samples investigated in this work, presented water uptake reduction up to 30% when going from 25 to 50°C.

Hence, the observed behavior in MFC films, already mentioned by Bedani et al. (2015), has to be related to the peculiar structure of MFC films, and it is likely produced by structural changes occurring during water sorption, which provide extra available sites after relaxation (swelling) of the cellulosic matrix.

That temperature effect can be quantitatively analyzed by calculating the molar enthalpy of mixing, $\Delta\tilde{H}_s$, from the experimental data, by considering an Arrhenius type correlation between logarithm of water solubility with the inverse of absolute. The enthalpy of mixing can be then obtained from solubility data by means of the following relationship:

$$\Delta\tilde{H}_s(\Omega_w) = R \left(\frac{\partial \ln(p/p^*)}{\partial (1/T)} \right)_{\Omega_w} \quad (5)$$

in which the derivative of water activity is taken considering data at different temperatures and water activities, but at constant water uptake.

As already pointed out above, the water sorption in nanocellulose systems is often described either as a physical adsorption process onto the fibers or fibrils, or as a penetrant dissolution in the amorphous regions of the material, or their combination. Interestingly, the same equation (Eq. 5) may account for the temperature dependence of water solubility for both mechanisms, with obvious differences in the meaning of the enthalpy change involved (enthalpy of mixing due to non-ideal mixing in the first case, heat of adsorption in the second one).

Indeed, the experimental solubility data obtained in this work follow the trend in Eq. 5 in the temperature range of 16 - 35 °C, and at water activities above 10% (corresponding to a water uptake of about 2 wt. % in both materials), at which the regression coefficient R^2 of water activity with the inverse of temperature at constant concentration is always higher than 0.9; the resulting values of $\Delta\tilde{H}_s$ in MFC G1 and MFC G2 are then reported in Table 1. Conversely, at lower R.H. no satisfactory analysis could be carried out, as the solubility data at different temperatures are too similar, in the order of the experimental error, and no reliable estimation of this quantity is possible. As one can see in Table 1, the enthalpy of mixing is a positive quantity, accounting for increased solubility at higher temperatures, as illustrated in Fig. 2 and 3; furthermore, it is an increasing function of water concentration, going from a value of 5.6 to 28.9 kJ/mol and from 17.7 to 27.5 kJ/mol, in MFC G1 and G2, respectively, when the water content increased from 0.020 to 0.045 g/g_{MFC}. The endothermic character of the sorption process is probably related to a significant relaxation of the cellulose nanofibrils, which produces an appreciable swelling of the matrix. In polymeric materials, the volume dilation

upon sorption is indeed a process that requires energy, as shown for example by Giacinti et al. (2005), even if its effect is usually covered by the exothermic character of the overall mixing process.

It is noteworthy that lower $\Delta\tilde{H}_s$ values are obtained for MFC G1 than for MFC G2 at the lowest RH considered for regression, but increasing the water content, the two materials behave similarly, approaching the same value. In the high activity range, indeed, water-water interactions, similar in MFC G1 and G2, become more frequent inside the matrix, thus reducing the differences between the water sorption mechanisms in the two materials.

Hence, the data suggest that after monolayer adsorption is completed the two materials request different amount of energy to relax and accommodate further incoming water molecules, which is higher for MGC G2, due to its higher surface charge with respect to MFC G1. Such differences are mainly relevant at low temperature and RH, when fiber are still closely packed and thermal energy is not sufficient to disrupt such interactions, and tend to vanish at higher water content, because in the swollen matrix short range interactions among fiber are not relevant anymore, as well as at higher temperatures (i.e. above 35°C), at which thermal vibration promotes such interactions making easier for water to enter the matrix. In this concern, it is worthwhile to note that the effect of the drying temperature previously discussed seems to be consistent with such analysis, as bound water is released at 35 °C, suggesting that such temperature is high enough to disrupt H-bonding on the surface of the fibers.

Table 1. Sorption enthalpies calculated for MFC G1 and MFC G2 between 16-35 °C.

Ω_w (g/g _{MFC})	MFC G1		MFC G2	
	$\Delta\tilde{H}_s$ (kJ/mol)	R ²	$\Delta\tilde{H}_s$ (kJ/mol)	R ²
0.020	5.64	0.995	17.74	0.957
0.030	12.09	1.000	19.48	0.900
0.040	21.46	0.954	25.84	0.998
0.045	27.43	0.999	26.10	0.999

4.3. Model analysis

As above mentioned, the obtained experimental data are analyzed by means of the Park and GAB models, suitable to the description of water solubility isotherms in these nanosized cellulosic materials. The characteristic model parameters are retrieved from the best fit of the solubility data, and the resulting values are summarized in Table 2, whereas Fig. 2 and Fig. 3 report the comparison between experiments and model calculations. A sole set of parameters, for each of the two models, is considered at 35 °C and higher temperatures, at which the sorption isotherms practically overlap. In all cases, both models can provide a very accurate representation of the water solubility in MFC systems (mean relative deviation well below 10%) with the same number of adjustable parameters (3), as the clustering contribution of the Park model has been neglected. Interestingly, the behavior of the two model is slightly different at 16 °C and 25 °C, while the two curves are practically coincident at above these temperatures.

Table 2. Park and GAB model solubility model parameters.

		Park			GAB			Ref.
	T (°C)	K_H	A_L	b_L	K_{ads}	C_m	C_G	
MFC G1	16	0.037	0.024	24	0.240	0.044	31.8	This work
	25	0.049	0.023	24	0.430	0.043	21.0	
	35-65	0.072	0.021	23	0.705	0.041	12.0	
MFC G2	16	0.053	0.019	19	0.160	0.064	19.9	This work
	25	0.068	0.018	19	0.319	0.063	11.6	
	35-65	0.104	0.017	20	0.615	0.059	8.0	
MFC G1	35	0.048	0.020	12	0.210	0.058	16.0	Minelli et al., 2010 *
MFC G2	35	0.090	0.021	21	0.510	0.062	10.0	
MFC	30	0.143	0.020	21	0.840	0.060	8.0	Aulin et al., 2010 *
MFC	25	0.115	0.021	22	0.720	0.060	8.0	Belbekhouche et al., 2011 *
flax fibers	25	0.116	0.013	59	0.784	0.048	9.5	Alix et al., 2009
flax fibers	25	0.114	0.021	47	0.892	0.036	59.6	Gouanvé et al., 2006

*Data are extracted from reference paper, and fit by Park and GAB models.

Park and GAB model parameters, K_H , A_L , b_L and K_{ads} , C_m , C_G , obtained in the present work are comparable to those presented in other studies on the water sorption in cellulosic fibers, suggesting very similar mechanisms for the water uptake in both MFC films considered before for solubility comparisons, whose model parameters are reported in Table 2. For example, Alix et al. (2009) as well as Gouanvé et al. (2006) reported Park and GAB parameters for water sorption in flax fibers obtaining values (included in Table 2) that are comparable with those here obtained for MFC samples. Slight changes in these parameters are likely due to different fitting procedures applied, and to different assumptions in the clustering term, neglected in this study (Alix et al., 2009; Belbekhouche et al., 2011; Bessadok et al., 2007, 2009; Gouanvé et al., 2006).

Considering more attentively Park model regression, it can be noticed that the parameters A_L and b_L , characteristic of Langmuir adsorption mechanisms (mainly relevant at low water activity), are almost temperature independent for both MFC G1 and MFC G2, indicating no significant changes in available sites for penetrating water molecules (A_L), and in the affinity parameter, b_L . No large differences are also observed among the two generations, as the obtained values for A_L and b_L are only slightly higher in MFC G1 than in MFC G2, in the order of the uncertainty arisen by the model parameter optimization procedure. Consequently, Park model suggests that the amount of adsorbed water on the fibrils surface is very similar for both MFC generations, and it is practically unaffected by temperature changes. On the other hand, the Henry's solubility coefficient (K_H) increased significantly with temperature for both MFC generations as the temperature increased from 16 to 35 °C; and its value is always higher for MFC G2 with respect to MFC G1, likely in view of the larger interfibrillar region accessible to penetrant molecules. Moreover, the carboxymethylation pretreatment of the cellulose pulp, which typically produces more hydrophilic structures, is characterized by larger values of K_H , accounting for water desolved in the amorphous, interfibrillar regions of the material.

A similar analysis can be carried out on the GAB model parameters, also useful to understand the water sorption mechanism in the two MFC types. The value of C_m , for example, represents the amount of water molecules adsorbed in the monolayer, and, as also showed for Langmuir parameter A_L , it is practically temperature independent. On the other hand, the analysis provided by the GAB model indicates a larger availability of sites for MFC G2, as C_m is significantly larger than in MFC G1, as expected due to the larger surface charge of these nanofibrils, although not well represented by the Park model, in which A_L parameter resulted always slightly higher in MFC G1 rather than in MFC G2. The two models, therefore, seem to suggest different weights of the monolayer adsorption in the two MFCs inspected, with GAB results seeming more reliable on the basis of material properties, although it is difficult to draw a final conclusion about this point, due to the very slight difference shown by the experimental data in the low activity range.

Noticeably, Park and GAB models agree in the description of the temperature dependence of water sorption. Similarly to K_H in Park model, C_G and K_{ads} are thermodynamic sound parameters, and are significantly temperature dependent (by means of a Van't Hoff relation) (Quirijns et al., 2005; Timmermann, 2003), as C_G defines the difference between the strength of bound water in the monolayer with that in the successive layer, whereas K_{ads} is the difference in enthalpy between the multilayer and bulk liquid. Based on their physical meaning, C_G is expected to decrease with temperature, while K_{ads} should increase. Such behavior is indeed observed for both materials, as K_{ads} increase of about 70% for the two MFCs going from 16 to 35°C, while in the same temperature range C_G decreases of about 60%. In agreement with their physical meaning, the observed variations are indeed of Van't Hoff type, and the resulting correlation factor R^2 is in the order of 0.99.

Therefore, both Park and GAB models can represent very well the observed solubility isotherms, although based on completely different approaches, with the description of the

physical mechanisms of water sorption in the investigate systems, likely involving both multilayer adsorption and physical dissolution. Based on the obtained results, no final conclusion can be made about the most suitable model to describe the data, and a preference, if any, can be given to GAB just because it is potentially able to describe possible upturn of the isotherm without the addition of any further parameter.

4.4. Diffusion kinetics

The kinetics of water diffusion in MFC films has been also recorded, and an example of the transient water uptake as function of the square root of time is reported in Fig. 7 and Fig. 8, for two generic water sorption steps in MFC G1 at 16 and 45 °C, at average relative humidity of 1%, 54% and 13%, 42%, respectively.

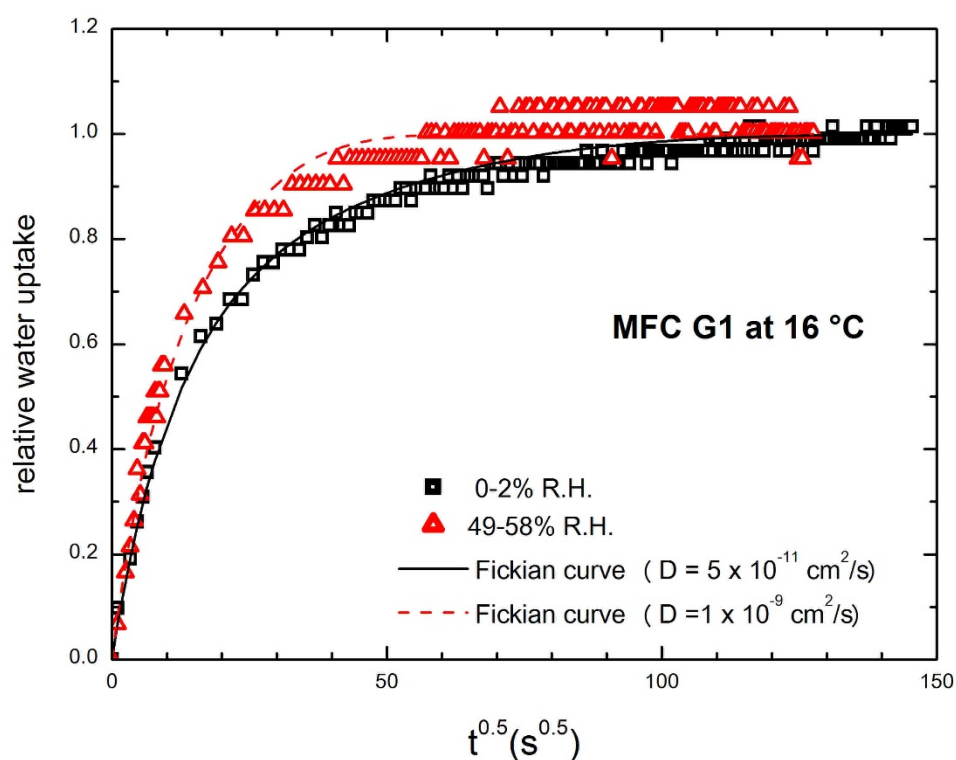


Figure 7. Mass uptake for MFC G1 at 16 °C, at low (0-2%) and high R.H. (49-58%).

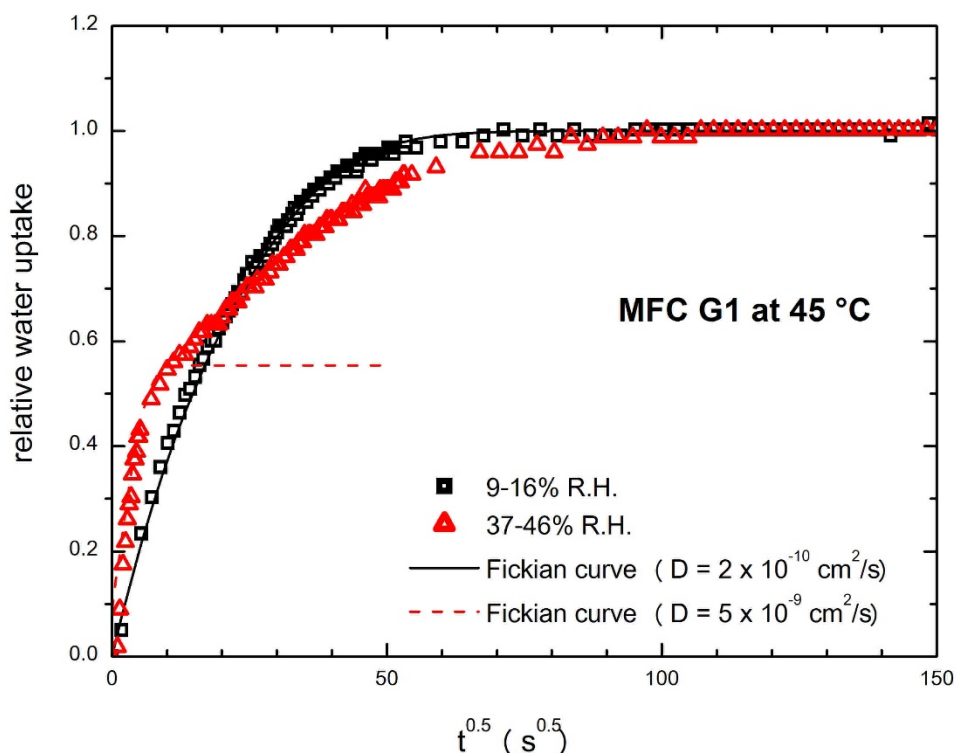


Figure 8. Mass uptake for MFC G1 at 45 °C at low (9-16%) and high R.H. (37-46%).

At low temperature, in the whole range of the water activity investigated in this work, the kinetics are well described by a simple Fickian model (Eq. 2), also included in Figures 7 and 8, and the diffusion coefficients can be readily determined from best fit of the experimental data, resulting e.g. in the values of $5.0 \cdot 10^{-11} \text{ cm}^2/\text{s}$ and $1.0 \cdot 10^{-9} \text{ cm}^2/\text{s}$ at 16 °C at the two activities reported in Fig. 7, and $2.0 \cdot 10^{-10} \text{ cm}^2/\text{s}$ for 13% of average water activity at 45 °C (Fig. 8). However, at 45 °C and above, at higher water activity, the sorption process shows a more complex behavior, which cannot be simply described by a sole diffusion mechanism, as a two stage non-Fickian kinetics is apparent. Only the curve at early times, covering roughly the initial 50-60% of the relative water uptake, is somewhat Fickian and characterized by a rather fast rate of diffusion ($D = 5.0 \cdot 10^{-9} \text{ cm}^2/\text{s}$).

These features have been found at all temperature values, with the only exceptions of 16 and 25 °C, at which no evident secondary process has been observed in the sorption kinetics,

leading therefore to a lower water uptake, as previously discussed. At the lower temperatures, apparently, this second mechanism that provides an extra-sorption contribution, has not been activated. In this concern, also the present kinetics data are consistent with the qualitative description of temperature dependence of solubility provided above; the non-Fickian behavior observed at high temperatures, indeed, is likely to be ascribed to an increased ability of the material to rearrange itself and to swell, accommodating more water with respect to what happens at the lower temperatures.

Such secondary process is probably related to pure relaxational phenomena occurring on the MFC matrix during sorption, as typically observed in glassy polymers with swelling penetrants (Berens & Hopfenberg, 1978), or to complex mechanisms of diffusion in the multiphase material, which includes basically 3 distinct phases, crystallites, amorphous phase and interfibrillar region, as illustrated by Belbekhouche et al. (2011), Bessadok et al. (2009) and Gouanvé et al. (2007), who accounted for two different diffusion coefficients to describe water diffusion in the MFC or cellulose fibers systems. Several works in the literature, however, make use of so-called Parallel Exponential Kinetics (PEK) kinetics, which assumes two not specific, parallel and independent first order processes occurring simultaneously, to describe water sorption kinetics (Belbekhouche et al., 2011; Kohler et al., 2003; Okubayashi et al., 2004).

The complete presentation of kinetic data and their detailed analysis however is outside the scope of the present work and will be presented in a future work.

5. Conclusion

The water vapor sorption behavior has been investigated in two types of microfibrillated cellulose (MFC) films, MFC G1 and G2, in wide ranges of temperature (16-65 °C), and water activity (0-0.70).

Depending on the pre-treatment procedure of the pristine pulp, the resulting films showed different properties, which played a significant role in the sorption experiments. Experimental analysis showed larger water solubilities in MFC G2 (carboxymethylation pretreatment) with respect to MFC G1 (enzymatic pretreatment), due to the higher surface charge and higher hydrophilic character of the microfibrils.

Overall, water solubility values measured for the two MFC materials were in line with those available in the open literature, and the typical behavior of the sorption isotherm in cellulosic materials was observed, with an initial downward curvature followed by a linear trend. The obtained solubility were modeled by two appropriate approaches, commonly applied to this aim for cellulosic materials, the Park and GAB model, that both proved to be able to consistently describe the observed experimental behavior.

Interestingly, the tests pointed out that the MFC samples need to be carefully evacuated from atmospheric moisture by conditioning treatment under vacuum, at temperatures higher than 35 °C, as only above this threshold, the procedure is effective in complete water removal. No temperature effect was observed on the solubility above 35 °C, while an appreciably lower uptake was obtained at 16 and 25 °C, resulting in an endothermic sorption process at temperature below 35 °C. Mixing enthalpies in the range of 5.6-27.5 kJ/mol and 17.7-26.1 kJ/mol were obtained for MFC G1 and MFC G2, respectively. Such unexpected result, likely related to the structural features of MFC films, points out once again the peculiar properties of nanocellulose with respect to other cellulose-based materials.

The analysis of the sorption kinetics revealed that the sorption process is substantially diffusive and well described by Fick's at lower activities and at lower temperatures. When the temperature is raised and the water content in the MFC film increases, a secondary process is also observed at longer times. This dual behavior is associated to the diffusion in a complex

622 multiphase medium and to some kind of structural relaxation of interfibrillar bonds occurring
623 in the matrix at large water uptakes.

624

625 **Acknowledgements**

626

627 The authors gratefully acknowledge financial support provided through the EU Seventh
628 Framework NEWGENPAK project and COST Action FP 1003 BioMatPack for the research
629 reported in this paper.

630

References

- Alix, S., Philippe, E., Bessadok, A., Lebrun, L., Morvan, C., & Marais, S. (2009). Effect of chemical treatments on water sorption and mechanical properties of flax fibres. *Bioresource Technology*, 100, 4742–4749. doi:10.1016/j.biortech.2009.04.067
- Al-Muhtaseb, A. H., McMinn, W. A. M., & Magee, T. R. A. (2004). Water sorption isotherms of starch powders: Part 1: Mathematical description of experimental data. *Journal of Food Engineering*, 61, 297–307. doi:10.1016/S0260-8774(03)00133-X
- Andresen, M., Stenstad, P., Møretro, T., Langsrud, S., Syverud, K., Johansson, L. S., & Stenius, P. (2007). Nonleaching antimicrobial films prepared from surface-modified microfibrillated cellulose. *Biomacromolecules*, 8, 2149–2155. doi:10.1021/bm070304e
- Aulin, C., Ahola, S., Josefsson, P., Nishino, T., Hirose, Y., Osterberg, M., & Wågberg, L. (2009). Nanoscale cellulose films with different crystallinities and mesostructures--their surface properties and interaction with water. *Langmuir : The ACS Journal of Surfaces and Colloids*, 25(13), 7675–7685. doi:10.1021/la900323n
- Aulin, C., Gällstedt, M., & Lindström, T. (2010). Oxygen and oil barrier properties of microfibrillated cellulose films and coatings. *Cellulose*, 17(3), 559–574. doi:10.1007/s10570-009-9393-y
- Azizi Samir, M. A. S., Alloin, F., & Dufresne, A. (2005). Review of recent research into cellulosic whiskers, their properties and their application in nanocomposite field. *Biomacromolecules*, 6(2), 612–26. doi:10.1021/bm0493685
- Bedane, A. H., Eić, M., Farmahini-Farahani, M., Xiao H. (2015). Water vapor transport properties of regenerated cellulose and nanofibrillated cellulose films. *J. Membr. Sci.* 493 (2015) 46–57.
- Belbekhouche, S., Bras, J., Siqueira, G., Chappey, C., Lebrun, L., Khelifi, B., ... Dufresne, A. (2011). Water sorption behavior and gas barrier properties of cellulose whiskers and microfibrils films. *Carbohydrate Polymers*, 83, 1740–1748. doi:10.1016/j.carbpol.2010.10.036
- Berens, A. ., & Hopfenberg, H. . (1978). Diffusion and relaxation in glassy polymer powders: 2. Separation of diffusion and relaxation parameters. *Polymer*. doi:10.1016/0032-3861(78)90269-0
- Berglund, L., (2005). Cellulose-based nanocomposites, in Natural Fibres, Biopolymers and Biocomposites, ed. A. K. Mohanty, M. Misra and L. T. Drzal, Taylor & Francis, Boca Raton, pp. 807–832.
- Bessadok, A., Langevin, D., Gouanvé, F., Chappey, C., Roudesli, S., & Marais, S. (2009). Study of water sorption on modified Agave fibres. *Carbohydrate Polymers*, 76, 74–85. doi:10.1016/j.carbpol.2008.09.033

- 667 Bessadok, A., Marais, S., Gouanvé, F., Colasse, L., Zimmerlin, I., Roudesli, S., & Métayer,
668 M. (2007). Effect of chemical treatments of Alfa (*Stipa tenacissima*) fibres on water-
669 sorption properties. *Composites Science and Technology*, 67, 685–697.
670 doi:10.1016/j.compscitech.2006.04.013
- 671 Brunauer, S., Emmett, P. H., & Teller, E. (1938). Gases i n Multimolecular Layers. *Journal of*
672 *the American Chemical Society*, 60, 309–319. doi:10.1021/ja01269a023
- 673 Crank, J., (1956). The Mathematics of Diffusion, *Clarendon Press*, Oxford.
- 674 De Angelis, M. G., Lodge, S., Giacinti Baschetti, M., Sarti, G. C., Doghieri, F., Sanguineti,
675 A., & Fossati, P. (2006). Water sorption and diffusion in a short-side-chain
676 perfluorosulfonic acid ionomer membrane for PEMFCS: effect of temperature and pre-
677 treatment. *Desalination*, 193, 398–404. doi:10.1016/j.desal.2005.06.070
- 678 Dufresne, A., Cavaillé, J. Y., (1998). Clustering and percolation effect in microcrystalline
679 starch reinforced thermoplastic. *J. Polym. Sci. Polym. Phys.*, 36, 2211–2224.
- 680 Dufresne, A. (2008). Polysaccharide nano crystal reinforced nanocomposites. *Canadian*
681 *Journal of Chemistry*. doi:10.1139/v07-152
- 682 Ferro-Fontan, C., Chirife, J., Sancho, E. Iglesias, H.A. (1982). Analysis of a model for
683 sorption phenomena in foods. *J. Food Sci.*, 47, 1590-1595.
- 684 Fukuzumi, H., Saito, T., Iwata, T., Kumamoto, Y., & Isogai, A. (2009). Transparent and high
685 gas barrier films of cellulose nanofibers prepared by TEMPO-mediated oxidation.
686 *Biomacromolecules*, 10, 162–165. doi:10.1021/bm801065u
- 687 Giacinti Baschetti, M., Ghisellini, M., Quinzi, M., Doghieri, F., Stagnaro, P., Costa, G., &
688 Sarti, G. C. (2005). Effects on sorption and diffusion in PTMSP and TMSP / TMSE
689 copolymers of free volume changes due to polymer ageing. *Journal of Molecular*
690 *Structure*, 739, 75–86. doi:10.1016/j.molstruc.2004.08.027
- 691 Gouanvé, F., Marais, S., Bessadok, A., Langevin, D., & Métayer, M. (2007). Kinetics of
692 water sorption in flax and PET fibers. *European Polymer Journal*, 43, 586–598.
693 doi:10.1016/j.eurpolymj.2006.10.023
- 694 Gouanvé, F., Marais, S., Bessadok, A., Langevin, D., Morvan, C., & Métayer, M. (2006).
695 Study of water sorption in modified flax fibers. *Journal of Applied Polymer Science*,
696 101, 4281–4289. doi:10.1002/app.23661
- 697 Guggenheim, E. A. (1966). *Application of statistical mechanics*. Oxford: UK: Clarendon
698 Press.
- 699 Halsey, G. (1948). Physical adsorption on non-uniform surfaces. *J. Chem. Phys.* 16, 931-937.
- 700 Henderson, S.M. (1952). A basic concept of equilibrium moisture. *Agr. Eng.* 33, 29-32.

- 701 Henriksson, M., Berglund, L. A., Isaksson, P., Lindström, T., & Nishino, T. (2008). Cellulose
702 nanopaper structures of high toughness. *Biomacromolecules*, 9, 1579–1585.
703 doi:10.1021/bm800038n
- 704 Herrick, F. W., Casebier, R. L., Hamilton, K. J., & Sandberg, K. R. (1983). Microfibrillated
705 Cellulose: Morphology and Accessibility. *Journal of Applied Polymer Science: Applied*
706 *Polymer Symposium*, 37, 797–813.
- 707 Hubbe, M. A., Rojas, O. J., Lucia, L. A., & Sain, M. (2008). CELLULOSIC
708 NANOCOMPOSITES: A REVIEW. *BioResources*. Retrieved from
709 [http://ojs.cnr.ncsu.edu/index.php/BioRes/article/view/BioRes_03_3_0929_Hubbe_RLS_](http://ojs.cnr.ncsu.edu/index.php/BioRes/article/view/BioRes_03_3_0929_Hubbe_RLS_Cellulosic_Nanocomposites_Rev)
710 [Cellulosic_Nanocomposites_Rev](http://ojs.cnr.ncsu.edu/index.php/BioRes/article/view/BioRes_03_3_0929_Hubbe_RLS_Cellulosic_Nanocomposites_Rev)
- 711 Iwatake, A., Nogi, M., & Yano, H. (2008). Cellulose nanofiber-reinforced polylactic acid.
712 *Composites Science and Technology*, 68, 2103–2106.
713 doi:10.1016/j.compscitech.2008.03.006
- 714 R. Jeffries. (1960). The sorption of water by cellulose and eight other textile polymers. J.
715 *Textile Inst. Trans.* 51, 339-374.
- 716 Johansson, C., Bras, J., Mondragon, I., Nechita, P., Plackett, D., Šimon, P., ... Aucejo, S.
717 (2012). Renewable fibers and bio-based materials for packaging applications - A review
718 of recent developments. *BioResources*.
- 719 Kamel, S. (2007). Nanotechnology and its applications in lignocellulosic composites, a mini
720 review. *eXPRESS Polymer Letters*, 1(9), 546–575.
721 doi:10.3144/expresspolymlett.2007.78
- 722 Kohler, R., Dück, R., Ausperger, B., & Alex, R. (2003). A numeric model for the kinetics of
723 water vapor sorption on cellulosic reinforcement fibers. *Composite Interfaces*.
724 doi:10.1163/156855403765826900
- 725 Lange, J., & Wyser, Y. (2003). Recent Innovations in Barrier Technologies for Plastic
726 Packaging - A Review. *Packaging Technology and Science*. doi:10.1002/pts.621
- 727 Lavoine, N., Desloges, I., Dufresne, A., & Bras, J. (2012). Microfibrillated cellulose - Its
728 barrier properties and applications in cellulosic materials: A review. *Carbohydrate*
729 *Polymers*. doi:10.1016/j.carbpol.2012.05.026
- 730 Leitner, J., Hinterstoisser, B., Wastyn, M., Keckes, J., & Gindl, W. (2007). Sugar beet
731 cellulose nanofibril-reinforced composites. *Cellulose*, 14, 419–425. doi:10.1007/s10570-
732 007-9131-2
- 733 Liu, A., Walther, A., Ikkala, O., Belova, L., & Berglund, L. A. (2011). Clay nanopaper with
734 tough cellulose nanofiber matrix for fire retardancy and gas barrier functions.
735 *Biomacromolecules*, 12, 633–641. doi:10.1021/bm101296z
- 736 Lu, J., Askeland, P., & Drzal, L. T. (2008). Surface modification of microfibrillated cellulose
737 for epoxy composite applications. *Polymer*, 49, 1285–1296.
738 doi:10.1016/j.polymer.2008.01.028

- 739 Lu, J., Wang, T., & Drzal, L. T. (2008). Preparation and properties of microfibrillated
740 cellulose polyvinyl alcohol composite materials. *Composites Part A: Applied Science*
741 *and Manufacturing*, 39(5), 738–746. doi:10.1016/j.compositesa.2008.02.003
- 742
- 743 Michaels, A. S., Vieth, W. R., & Barrie, J. A. (1963). Solution of gases in polyethylene
744 terephthalate. *Journal of Applied Physics*, 34, 1–12. doi:10.1063/1.1729066
- 745 Mihranyan, A., Llagostera, A. P., Karmhag, R., Strømme, M., & Ek, R. (2004). Moisture
746 sorption by cellulose powders of varying crystallinity. *International Journal of*
747 *Pharmaceutics*, 269, 433–442. doi:10.1016/j.ijpharm.2003.09.030
- 748 Minelli, M., Baschetti, M. G., Doghieri, F., Ankerfors, M., Lindström, T., Siró, I., & Plackett,
749 D. (2010). Investigation of mass transport properties of microfibrillated cellulose (MFC)
750 films. *Journal of Membrane Science*, 358(1-2), 67–75.
751 doi:10.1016/j.memsci.2010.04.030
- 752 Minelli, M., De Angelis, M. G., Doghieri, F., Rocchetti, M., & Montenero, A. (2010). Barrier
753 Properties of Organic – Inorganic Hybrid Coatings Based on Polyvinyl Alcohol With
754 Improved Water Resistance. *Polymer Engineering and Science*, 50(1), 144–153.
755 doi:10.1002/pen
- 756 Morton, W. E., & Hearle, J. W. S. (1993). *Physical properties of textile fibres*. New York
757 1993.
- 758 Nogi, M., Iwamoto, S., Nakagaito, A. N., & Yano, H. (2009). Optically Transparent
759 Nanofiber Paper. *Advanced Materials*, 21, 1595–1598. doi:10.1002/adma.200803174
- 760 Okubayashi, S., Griesser, U. J., & Bechtold, T. (2004). A kinetic study of moisture sorption
761 and desorption on lyocell fibers. *Carbohydrate Polymers*.
762 doi:10.1016/j.carbpol.2004.07.004
- 763 Osterberg, M., Vartiainen, J., Lucenius, J., Hippel, U., Seppälä, J., Serimaa, R., & Laine, J.
764 (2013). A fast method to produce strong NFC films as a platform for barrier and
765 functional materials. *ACS Applied Materials & Interfaces*, 5(11), 4640–7.
766 doi:10.1021/am401046x
- 767 Oswin, C.R. (1946) The kinetics of package life III. The isotherm. *J. Chem. Ind.* 65, 419–421.
- 768 Pääkkö, M., Ankerfors, M., Kosonen, H., Nykänen, A., Ahola, S., Österberg, M., ...
769 Lindström, T. (2007). Enzymatic hydrolysis combined with mechanical shearing and
770 high-pressure homogenization for nanoscale cellulose fibrils and strong gels.
771 *Biomacromolecules*, 8, 1934–1941. doi:10.1021/bm061215p
- 772 Peleg, M. (1993). Assessment of a semi-empirical four parameter general model for sigmoid
773 moisture sorption isotherms. *J. Food Process Engineering*, 16, 21-37.
- 774 Plackett, D., Anturi, H., Hedenqvist, M., Ankerfors, M., Gällstedt, M., Lindström, T., & Siró,
775 I. (2010). Physical properties and morphology of films prepared from microfibrillated

- 776 cellulose and microfibrillated cellulose in combination with amylopectin. *Journal of*
777 *Applied Polymer Science*, 117, 3601–3609. doi:10.1002/app.32254
- 778 Quirijns, E. J., Van Boxtel, A. J. B., Van Loon, W. K. P., & Van Straten, G. (2005). Sorption
779 isotherms, GAB parameters and isosteric heat of sorption. *Journal of the Science of Food*
780 *and Agriculture*, 85, 1805–1814. doi:10.1002/jsfa.2140
- 781 Rouquerol, J., Avnir, D., Fairbridge, C. W., Everett, D. H., Haynes, J. H., Pernicone, N., ...
782 Unger, K. K. (1994). Recommendations for the characterization of porous solids. *Pure &*
783 *Appl. Chem*, 66, 1739–1758.
- 784 Siqueira, G., Bras, J., & Dufresne, A. (2009). Cellulose whiskers versus microfibrils:
785 influence of the nature of the nanoparticle and its surface functionalization on the
786 thermal and mechanical properties of nanocomposites. *Biomacromolecules*, 10(2), 425–
787 32. doi:10.1021/bm801193d
- 788 Siró, I., Plackett, D., Hedenqvist, M., Ankerfors, M., & Lindström, T. (2011). Highly
789 transparent films from carboxymethylated microfibrillated cellulose: The effect of
790 multiple homogenization steps on key properties. *Journal of Applied Polymer Science*,
791 119, 2652–2660. doi:10.1002/app.32831
- 792 Siroka, B., Noisternig, M., Griesser, U. J., & Bechtold, T. (2008). Characterization of
793 cellulosic fibers and fabrics by sorption/desorption. *Carbohydrate Research*, 343, 2194–
794 2199. doi:10.1016/j.carres.2008.01.037
- 795 Smith, S.E. (1947). The sorption of water vapour by high polymers J. Amer. Chem. Soc.
796 69,646-649.
- 797 Stenstad, P., Andresen, M., Tanem, B. S., & Stenius, P. (2008). Chemical surface
798 modifications of microfibrillated cellulose. *Cellulose*, 15, 35–45. doi:10.1007/s10570-
799 007-9143-y
- 800 Svagan, A. J., Azizi Samir, M. A. S., & Berglund, L. A. (2007). Biomimetic polysaccharide
801 nanocomposites of high cellulose content and high toughness. *Biomacromolecules*, 8,
802 2556–2563. doi:10.1021/bm0703160
- 803 Syverud, K., & Stenius, P. (2009). Strength and barrier properties of MFC films. *Cellulose*,
804 16, 75–85. doi:10.1007/s10570-008-9244-2
- 805 Timmermann, E. O. (2003). Multilayer sorption parameters: BET or GAB values? *Colloids*
806 *and Surfaces A: Physicochemical and Engineering Aspects*, 220(1-3), 235–260.
807 doi:10.1016/S0927-7757(03)00059-1
- 808 Turbak, A. F., Snyder, F. W., & Sandberg, K. R. (1983). Microfibrillated cellulose, a new
809 cellulose product: Properties, uses, and commercial potential. *Journal of Applied*
810 *Polymer Science: Applied Polymer Symposium*, 37, 815–827.
- 811 Velázquez de la Cruz, G., Torres, J.A., Martín-Polo, M.O. (2001) Temperature effect on the
812 moisture sorption isotherms for methylcellulose and ethylcellulose films. *Journal of Food*
813 *Engineering*, 48, 91-94

814

815 Vieth, W. ., & Sladek, K. . (1965). A model for diffusion in a glassy polymer. *Journal of*
816 *Colloid Science*. doi:10.1016/0095-8522(65)90071-1

817 Wågberg, L., Decher, G., Norgren, M., Lindström, T., Ankerfors, M., & Axnäs, K. (2008).
818 The build-up of polyelectrolyte multilayers of microfibrillated cellulose and cationic
819 polyelectrolytes. *Langmuir : The ACS Journal of Surfaces and Colloids*, 24(3), 784–95.
820 doi:10.1021/la702481v

821 Zimmermann, T., Pöhler, E., & Geiger, T. (2004). Cellulose fibrils for polymer
822 reinforcement. *Advanced Engineering Materials*, 6(9), 754–761.

823 Zografi, G., Kontny, M. J., Yang, A. Y. S., & Brenner, G. S. (1984). Surface area and water
824 vapor sorption of microcrystalline cellulose. *International Journal of Pharmaceutics*, 18,
825 99–116. doi:10.1016/0378-5173(84)90111-X

826